THE JOURNAL OF BIOLOGICAL CHEMISTRY VOL. 283, NO. 7, pp. 4145–4154, February 15, 2008

Dimeric Structure of Human Na^+/H^+ Exchanger Isoform 1 Overproduced in *Saccharomyces cerevisiae*[*]

Received for publication, June 12, 2007, and in revised form, November 8, 2007 Published, JBC Papers in Press, December 12, 2007, DOI 10.1074/jbc.M704844200

Karine Moncoq[1], **Grant Kemp**[1], **Xiuju Li, Larry Fliegel**[2], **and Howard S. Young**[3]

From the Department of Biochemistry, University of Alberta, Edmonton, Alberta T6G 2H7, Canada

The Na^+/H^+ exchanger isoform 1 (NHE1) is an integral membrane protein that regulates intracellular pH by extruding an intracellular H^+ in exchange for one extracellular Na^+. The human NHE1 isoform is involved in heart disease and cell growth and proliferation. Although details of NHE1 regulation and transport are being revealed, there is little information available on the structure of the intact protein. In this report, we demonstrate overexpression, purification, and characterization of the human NHE1 (hNHE1) protein in *Saccharomyces cerevisiae*. Overproduction of the His-tagged protein followed by purification via nickel-nitrilotriacetic acid-agarose chromatography yielded 0.2 mg of pure protein/liter of cell culture. Reconstitution of hNHE1 in proteoliposomes demonstrated that the protein was active and responsive to an NHE1-specific inhibitor. Circular dichroism spectroscopy of purified hNHE1 revealed that the protein contains 41% α-helix, 23% β-sheet, and 36% random coil. Size exclusion chromatography indicated that the protein-detergent micelle was in excess of 200 kDa, consistent with an hNHE1 dimer. Electron microscopy and single particle reconstruction of negatively stained hNHE1 confirmed that the protein was a dimer, with a compact globular domain assigned to the transmembrane region and an apical ridge assigned to the cytoplasmic domain. The transmembrane domain of the hNHE1 reconstruction was clearly dimeric, where each monomer had a size and shape consistent with the predicted 12 membrane-spanning segments for hNHE1.

The Na^+/H^+ exchanger isoform-1 (NHE1)[4] is a ubiquitously expressed plasma membrane glycoprotein. It extrudes a single intracellular proton in exchange for one extracellular sodium and thereby functions to protect cells from intracellular acidification while facilitating extracellular Na^+ entry into the cytosol (1). NHE1 was the first isoform discovered and a total of nine isoforms of the Na^+/H^+ exchanger have been identified to date, designated NHE1-NHE9 (2). While NHE1 appears to be the housekeeping isoform, isoforms NHE2-NHE9 have more limited tissue distributions and some have predominantly intracellular localization (reviewed in Ref. 3). The Na^+/H^+ exchanger consists of two domains, a membrane domain of ~500 amino acids and a 315 amino acid C-terminal cytosolic domain. The membrane domain carries out ion transport and is regulated by the cytosolic domain in response to phosphorylation and several accessory proteins that bind to this domain. Phosphorylation occurs within the last 178 amino acids (4, 5) and a number of proteins bind throughout the cytosolic domain and regulate NHE1 activity (reviewed in Ref. 6).

Mammalian NHE1 plays a key role in regulation of cell pH, cell volume, cell proliferation, and metastasis in some types of tumor cells (1, 6–10). The NHE1 isoform of the Na^+/H^+ exchanger plays a critical role in several forms of heart disease, mediating the damage that occurs with ischemia/reperfusion of the heart (8–10) and being an important mediator of myocardial hypertrophy (6). Clinical trials are attempting to develop NHE1 inhibitors for treatment of various forms of heart disease (11), though serious concerns have been raised about the isoform specificity of the inhibitors in some clinical trials (12). This suggests that an improved knowledge of NHE1 structure might be desirable in the design of improved inhibitors.

The lack of a natural source of NHE1 protein required the development of an overproduction system to begin structural studies. Though we have had some success in high level expression and structural analysis of isolated transmembrane segments of the mammalian NHE1 protein (13), this has remained a difficult undertaking and *Escherichia coli* seems resistant to expression of larger transmembrane fragments of eukaryotic Na^+/H^+ exchangers (14). The successful use of other microbial expressions systems include x-ray crystallographic structures of a rat brain voltage-dependent potassium channel overproduced in *Pichia pastoris* (15, 16) and a rabbit sarcoplasmic reticulum Ca^{2+}-ATPase overproduced in *Saccharomyces cerevisiae* (17, 18). In addition, mammalian Na^+/H^+ exchanger isoforms have been previously expressed in *S. cerevisiae*, though only in relatively small amounts with NHE1 expressed either as a functionally inactive or mistargeted protein (19–21). These results suggested that *S. cerevisiae* might be a suitable host for large scale NHE1 overexpression. Herein we describe the expression and characterization of the NHE1 isoform of the Na^+/H^+ exchanger in this microbial system, following an approach similar to that used for overproduction of an anion exchanger (AE1 or Band 3) in *S. cerevisiae* (22). Our results show that this system can be used to produce milligram quantities of human NHE1 (hNHE1), where

* This work was supported in part by grants from the Canadian Institutes of Health Research (to H. S. Y. and L. F.). The costs of publication of this article were defrayed in part by the payment of page charges. This article must therefore be hereby marked "*advertisement*" in accordance with 18 U.S.C. Section 1734 solely to indicate this fact.

[1] Supported by the Canadian Institutes of Health Research Strategic Training Initiative in Membrane Proteins and Cardiovascular Disease. Both authors have contributed equally to this work.

[2] Supported by an Alberta Heritage Foundation for Medical Research Scientist Award.

[3] Supported by an Alberta Heritage Foundation for Medical Research Senior Scholar Award. To whom correspondence should be addressed. E-mail: hyoung@ualberta.ca.

[4] The abbreviations used are: NHE1, Na^+/H^+ exchanger isoform 1; LPC, L-α-lysophosphatidylcholine; DDM, *n*-dodecyl β-D-maltoside; FC, Fos-choline; MES, 4-morpholineethanesulfonic acid; NTA, nitrilotriacetic acid; hNHE1, human NHE1.

the protein is easily purified from membranes, is fully functional in reconstituted vesicles, and is suitable for structural studies. Single particle electron microscopy of the detergent-solubilized, purified hNHE1 protein reveals a compact dimer at 22-Å resolution. These data provide the first structural insight into hNHE1 and its oligomeric state.

EXPERIMENTAL PROCEDURES

Materials—Biochemicals were from Sigma unless specified otherwise. TaqDNA polymerase was purchased from Invitrogen. DNA restriction and modification enzymes were from New England BioLabs (Beverly, MA). Products for culture of *S. cerevisiae* were purchased from DIFCO Media Products. Ni-NTA-agarose was purchased from Qiagen (Valencia, CA), calmodulin-agarose resin, Sephadex G-50, and Superdex 200 HR 10/30 were from Amersham Biosciences (Piscataway, NJ). The detergents octaethylene glycol mono-*n*-dodecyl ether ($C_{12}E_8$), *n*-dodecyl β-D-maltoside (DDM), and Fos-choline (FC) 10, 12, and 14 were purchased from Anatrace (Maumee, OH). L-α-lysophosphatidylcholine (LPC) and egg-yolk L-α-phosphatidylcholine (EYPC) were from Avanti Polar Lipids (Alabaster, AL). Bio-Beads (SM-2) were from Bio-Rad. HisProbe-HRP was from Pierce, anti-NHE1 monoclonal antibody was from Chemicon Int. Inc. (Temecula, CA). The *S. cerevisiae* W303.1b strain (*a, leu2, his3, trp1, ura3, ade2–1, can^r, cir$^+$*) and the expression plasmid pYeDP60 were generously supplied by Denis Pompon (CGM, Gif-sur-Yvette, France).

Site-directed Mutagenesis and Plasmid Construction—The cDNA of hNHE1 was obtained from the pYN4+ plasmid containing the entire coding region (13). Site-directed mutagenesis was initially performed using amplification with PWO DNA polymerase (Roche Applied Sciences) followed by use of the Stratagene (La Jolla, CA) QuikChange™ site-directed mutagenesis kit as recommended by the manufacturer. Mutations were designed to create a new restriction enzyme site for use in screening transformants. The mutant plasmid pYN4-N75D was created with the primers GAGCCGCCCTGTcgAcCATTCCGTCACTG, CAGTGACGGAATGgTcgACAGGGCGGCTC to remove the nonessential glycosylation site at amino acid Asn^{75}. Prior to cloning into the yeast expression plasmid pYeDP60, the unique BglII restriction site present in the coding sequence of hNHE1 in pYN4-N75D was also removed by site-directed mutagenesis using the primers 5′-CGCACCCCCTTCGAAATCTCCCTCTGG-3′ and 5′-CCAGAGGGAGATTTCGAAGGGGGTGCG-3′. The hNHE1-N75D gene was then amplified by PCR using TaqDNA polymerase with the appropriate primers 5′-GGAT*AGATCT*-ATGGTTCTGCGGTCTGGCATCTGTGGCCTC-3′ (forward), and 5′-CCAT*GGTACC***TCA**ATGATGATGATGATG-ATGATGATGATGATGACCACCCTGCCCCTTGGGGAA-GAACGGTTCTC-3′ (reverse), incorporating BglII and KpnI restriction sites respectively (italic) and a C-terminal "Gly_2His_{10}" tag (underlined) followed by a stop codon (bold). This amplified fragment was inserted in-frame into the plasmid pYeDP60 after cleavage of the BamHI and KpnI restriction sites. Restriction enzyme digestion and DNA sequencing verified the construct. The resultant construct was under control of the inducible GAL10-CYC1 hybrid promoter and the phosphoglycerate kinase terminator.

Yeast Transformation, Expression, and Culture—The yeast strain W303.1b was transformed using a high efficiency lithium acetate procedure (23) and selected on glucose minimal medium. For large scale expression, yeast cells were inoculated into selective medium (0.67% yeast nitrogen base, 2% glucose, 0.5% casamino acids, supplemented with 40 mg/liter Trp) and grown overnight at 30 °C. A 1:50 dilution was made into YPDE-2 medium (2% yeast extract, 1% glucose, 2% bactopeptone, 2.7% ethanol) and cells were grown at 28 °C with shaking until an A_{600} of 8.0 was obtained (~24–36 h). The expression of recombinant hNHE1 was induced by addition of galactose to a final concentration of 2% (w/v) for 12–14 h. After induction, cells were harvested yielding ~25 g wet cells per liter of culture.

Preparation of Membrane Fractions—Membrane fractions were prepared immediately from fresh culture (Fig. 1*A*). All manipulations of membrane fractions and purified protein were carried out at 4 °C or on ice. After 12–14 h induction, cells were collected by centrifugation at 5,000 × *g* for 15 min. The pellet was resuspended in cold water and centrifuged again. The pellet was then resuspended in ice-cold lysis buffer (25 mM HEPES-KOH pH 7.5, 1.5 M sorbitol, 1 mM EGTA, 1 mM EDTA, 1 mM dithiothreitol supplemented with 1 mM phenylmethylsulfonyl fluoride, 2 μg/ml leupeptin, 2 μg/ml aprotinin, 1 μg pepstatin) at a concentration of 0.6 g wet cells/ml. Cells were disrupted using a microfluidizer (Emulsiflex C3, Avestin Inc.) with 7 passes at 20,000 psi. The crude extract (CE) was centrifuged at 2,500 × *g* for 15 min to give a supernatant ($S_{2.5}$) and pellet ($P_{2.5}$). The $P_{2.5}$ pellet was suspended in an identical volume of lysis buffer and centrifuged again at 2,500 × *g* for 15 min to give a pellet (P) corresponding to cell debris and a supernatant ($S'_{2.5}$). The $S_{2.5}$ supernatant was centrifuged at 12,000 × *g* for 15 min. The pellet (P_{12}) was combined with the $S'_{2.5}$ supernatant and centrifuged at 12,000 × *g* for 15 min (P2). The resultant S_{12} and S'_{12} supernatants were pooled (S2) and centrifuged at 125,000 × *g* for 60 min in a Beckman Ti45 rotor. The final high speed pellet (P3) contained the membrane fractions enriched in hNHE1. The membrane fractions were resuspended in storage buffer (25 mM HEPES-KOH pH 7.5, 20% glycerol) at a protein concentration of ~15 mg/ml. The yield of membranes was about 300 mg of total protein per liter of culture. Membrane fractions were frozen in liquid nitrogen and stored at −80 °C until use.

Solubilization and Purification of hNHE1—Prior to solubilization and hNHE1 purification, membrane fractions were stripped of peripheral membrane proteins by treating with high ionic strength solution. This step was essential for enhanced purity of the final protein. Membrane fractions (12 mg/ml) were rapidly thawed to 4 °C and diluted 6 times in cold stripping buffer (60 mM Tris-HCl, pH 8.0, 12% glycerol, 0.7 M KCl). The suspension was then centrifuged at 125,000 × *g* for 60 min in a Ti45 rotor. The pellet was resuspended in storage buffer at ~4 mg/ml.

Initial solubilization of the stripped membranes used the detergents LPC, DDM, $C_{12}E_8$ and Fos-choline (FC-10, FC-12, and FC-14) at a protein concentration of 2 mg/ml and detergent/protein ratios of 1:1 to 5:1. Solubilization was carried out for 30 min followed by centrifugation at 100,000 × *g* for 30 min. The amount of hNHE1 solubilized was estimated from aliquots

withdrawn before and after centrifugation by Western blot analysis and detection with HisProbe-HRP. For large scale preparative solubilization of hNHE1, 1 volume of stripped membranes (4 mg/ml) was added to an equal volume of 1.2% FC-14 (w/v) or 1.2% LPC (w/v) in solubilization buffer (25 mM HEPES-KOH pH 7.5, 20% glycerol, 100 mM NaCl, 5 mM imidazole). The suspension was incubated for 30 min with constant, gentle stirring. Insoluble material was removed by centrifugation at 125,000 × *g* for 30 min.

For purification of hNHE1, the supernatant from detergent solubilization was applied at 0.5 ml/min to a Ni-NTA-agarose resin equilibrated in Ni-NTA binding buffer (25 mM HEPES-KOH pH 7.5, 20% glycerol, 100 mM NaCl, 5 mM imidazole, 0.1% detergent). The column was washed at 0.5 ml/min first with 4 column volumes of Ni-NTA wash buffer (25 mM HEPES-KOH pH 7.5, 20% glycerol, 100 mM NaCl, 10 mM imidazole, and 0.05% detergent), and then with four volumes of wash buffer containing 50 mM imidazole. hNHE1 was then eluted with 250 mM imidazole in Ni-NTA wash buffer with a flow rate at 0.2 ml/min. This purification procedure could be carried out using the detergents LPC, FC-14, or DDM. The hNHE1 resulting from this purification procedure was used for all structure and function described herein, with the exception of the circular dichroism (CD) spectroscopy studies.

For CD spectroscopy, the eluted protein was further purified using a calmodulin-Sepharose resin. To reduce the imidazole concentration, the Ni-NTA eluate was dialyzed overnight against binding buffer (25 mM HEPES-KOH 7.5, 20% glycerol, 100 mM NaCl, 4 mM $CaCl_2$, 0.05% FC-14). The dialyzed suspension was loaded onto a 1 ml calmodulin Sepharose column equilibrated with binding buffer at a flow rate of 0.5 ml/min. After washing with 3 column volumes of binding buffer, the protein was eluted with 2 volumes of elution buffer (25 mM HEPES-KOH 7.5, 20% glycerol, 100 mM NaCl, 5 mM EGTA, 0.05% FC-14) at a flow rate of 0.2 ml/min.

Biophysical and Biochemical Characterization of hNHE1—Size exclusion chromatography was used to examine the hydrodynamic volume of hNHE1. Samples of purified hNHE1 were run on a Superdex 200 HR 10/30 gel filtration column in 25 mM HEPES-KOH pH 7.5, 100 mM NaCl, 10% glycerol, 0.05% FC-14. The column was calibrated by measuring the elution volumes of proteins of known apparent molecular mass: thyroglobulin 679,000 (void volume); myosin, 200,000; bovine serum albumin, 66,000; carbonic anhydrase, 29,000; cytochrome *c*, 12,400.

Reconstitution of NHE1 into proteoliposomes followed established protocols (24). Briefly, 2.34 mg of egg yolk PC was dried to a thin film under nitrogen gas, and lyophilized. Dried lipids were mixed with reconstitution buffer (20 mM BTP-MES pH 7.5, 25 mM $(NH_4)_2SO_4$, 10% glycerol, supplemented with the fluorescent pH indicator 2.5 mM pyranine), 20 μl of 20% *n*-octyl-D-glucoside and 10 μg of purified hNHE1 to a final volume of 220 μl. The solubilized protein/lipid/detergent mixture was applied to a 2-ml Sephadex G-50 column that was preloaded with reconstitution buffer containing pyranine. The column eluate was incubated for 30 min at room temperature with 100 mg of wet SM-2 Bio-Beads to remove excess detergent. The sample was again applied to a 2-ml Sephadex G-50 column that was equilibrated with reconstitution buffer without pyranine. The resultant proteoliposomes containing hNHE1 were monitored for Na^+/H^+ exchanger activity via pyranine fluorescence using a PTI Deltascan spectrofluorometer with an excitation wavelength of 463 nm and an emission wavelength of 510 nm. Proteoliposomes containing hNHE1 (100 μl) and control liposomes (100 μl) were incubated at 25 °C, followed by dilution into a 2-ml reaction cuvette containing ammonium-free reconstitution buffer (20 mM BTP-MES pH 7.5, 10% glycerol) to generate a pH gradient. NaCl was added to initiate Na^+/H^+ exchange, which was monitored by the increase in pyranine fluorescence. The relative hNHE1 activities were measured by regression fitting of a 20 s linear region of the fluorescence intensity curves. For instance, the fluorescence curve in Fig. 4*A* was fit from 40 to 60 s yielding a change in fluorescence intensity of 7400 per second (set to 100% relative hNHE1 activity).

For CD spectroscopy, purified hNHE1 protein was exchanged into phosphate buffer (20 mM phosphate pH 7.5, 10% glycerol, 0.05% Fos-14) by overnight dialysis. CD was performed at 20 °C on a Jasco J-500C spectropolarimeter (Jasco, Easton, MD) (25). CD spectra were recorded from 250 to 190 nm in quartz cells (path length of 0.05 cm) as the average of 8 scans at 0.1 nm intervals. Protein concentration was determined by amino acid analysis (0.85 μM), and the CD spectrum obtained in millidegrees was converted to molar ellipticity and analyzed using CDPro (26).

For SDS-PAGE and Western blotting, protein samples were heated at 65 °C for 3 min and were separated on 10% SDS-polyacrylamide gels as described (27). For Western blot analysis, SDS-PAGE gels were transferred onto nitrocellulose membranes, and detection of recombinant hNHE1 was with His-Probe-HRP using the Supersignal West HisProbe Kit (Pierce) according to the manufacturer's instructions. Alternatively, a monoclonal anti-NHE1 antibody was used as the primary antibody as described earlier (27) and peroxidase-conjugated goat anti-mouse antibody (Pierce) was used as a secondary antibody. X-ray films were digitized with an Epson (Toronto, ON) Perfection 3200 densitometer and bands were quantified using ImageQuant software (GE Healthcare Life Sciences).

Protein concentrations were determined for yeast membrane preparations using a Lowry assay and for purified protein using an Amido Black assay (28, 29) with bovine serum albumin as standard.

Single Particle Electron Microscopy—Purified hNHE1 was diluted with 1% trehalose, 3% ammonium molybdate (pH 7.0) from an initial concentration of 0.2 mg/ml to a concentration of 0.01 mg/ml. Immediately following dilution, five microliters were pipetted onto a glow-discharged, carbon-coated grid for 30 s. The grid was washed with one drop of 2% uranyl acetate, and then allowed to sit on a drop of 2% uranyl acetate for 1 min. The excess stain was blotted with filter paper, and the grid was allowed to air dry. Data were collected on a Tecnai F20 (FEI Company) located in the Microscopy and Imaging Facility at the University of Calgary (Calgary, Alberta, Canada). The microscope was operated at 200 keV and images were recorded on Kodak SO-163 film under low-dose conditions at a magnification of 50,000× with a defocus ranging from −2.0 μm to −2.5 μm. Micrographs were digitized with a Nikon Super Coolscan 9000 with a scanning resolution of 6.35 μm/pixel,

followed by pixel averaging to achieve a final resolution of 5.08 Å/pixel.

Image processing and reconstruction were carried out using both EMAN (30) and SPIDER (31) software packages. Using EMAN's boxer, 7,930 particles were selected semi-automatically from 24 micrographs with a box size of 50 × 50 pixels. The boxed images were corrected for the CTF using ctfit (EMAN). Reference-free classification into 135 groups proceeded using startnrclasses (EMAN) and AP CA (SPIDER). The class averages generated by EMAN and SPIDER were combined into a common set of 44 groups using classesbymra (EMAN). A set of Euler angles was then assigned to these class averages (startAny command in EMAN; OP command in SPIDER), and initial three-dimensional models were built using common lines in Fourier space. These models were low pass filtered to 20 Å resolution, aligned and averaged (align3d and avg3d commands in EMAN). The average was taken as a preliminary model for 5 iterations of refinement in EMAN and SPIDER. A resolution of 22 Å of the final reconstruction was determined by calculating the Fourier shell correlation between two independent half datasets (eotest command in EMAN; 0.5 FSC criterion). Comparison of the final reconstruction with the predicted molecular mass for recombinant hNHE1 (92 kDa) indicated that the structure represented an hNHE1 dimer. 2-Fold symmetry was apparent and was applied to the final reconstruction (align3dsym and proc3d commands in EMAN).

RESULTS

Expression of Human NHE1 in S. cerevisiae and Preparation of Membrane Fractions—To obtain suitable amounts of functional protein for structural studies we expressed hNHE1 (amino acids 1–815) in a heterologous expression system (the yeast *S. cerevisiae*). The *N*-linked glycosylation of hNHE1 occurs at Asn^{75} and *O*-linked glycosylation occurs within the first extracellular loop (32). As glycosylation represents a potential obstacle to crystallization, we generated a mutant in which the *N*-linked glycosylation site was abolished (N75D). It has previously been shown that *N*-linked glycosylation of hNHE1 is not required for either cation exchange activity or biosynthesis of the protein (32, 33). In addition to this mutation, a dodecapeptide Gly_2His_{10} was introduced at the C terminus of hNHE1 to facilitate protein purification. Thus, a His-tagged hNHE1 N75D gene was inserted into the expression vector pYeDP60 (34) with a galactose inducible promoter. This expression system has previously been shown to be suitable for the heterologous expression of rabbit SERCA1a Ca^{2+}-ATPase (18) and the plant plasma membrane H^+-ATPase (35).

A differential centrifugation procedure was used to prepare membrane fractions that were enriched in hNHE1 (Fig. 1*A* and Table 1). Western blot analysis of the fractionated membranes illustrated the profile of hNHE1 yield in the various fractions (Fig. 1*B*). The expressed recombinant hNHE1 migrated on SDS-PAGE slightly lower than the 100-kDa standard, which is in good agreement with the predicted molecular weight of 92 kDa for the unglycosylated protein. The P3 light membranes (corresponding to endoplasmic reticulum and secretion vesicles) contained most of the hNHE1 protein, while the heavy P2 membranes (plasma membranes and mitochondria) contained

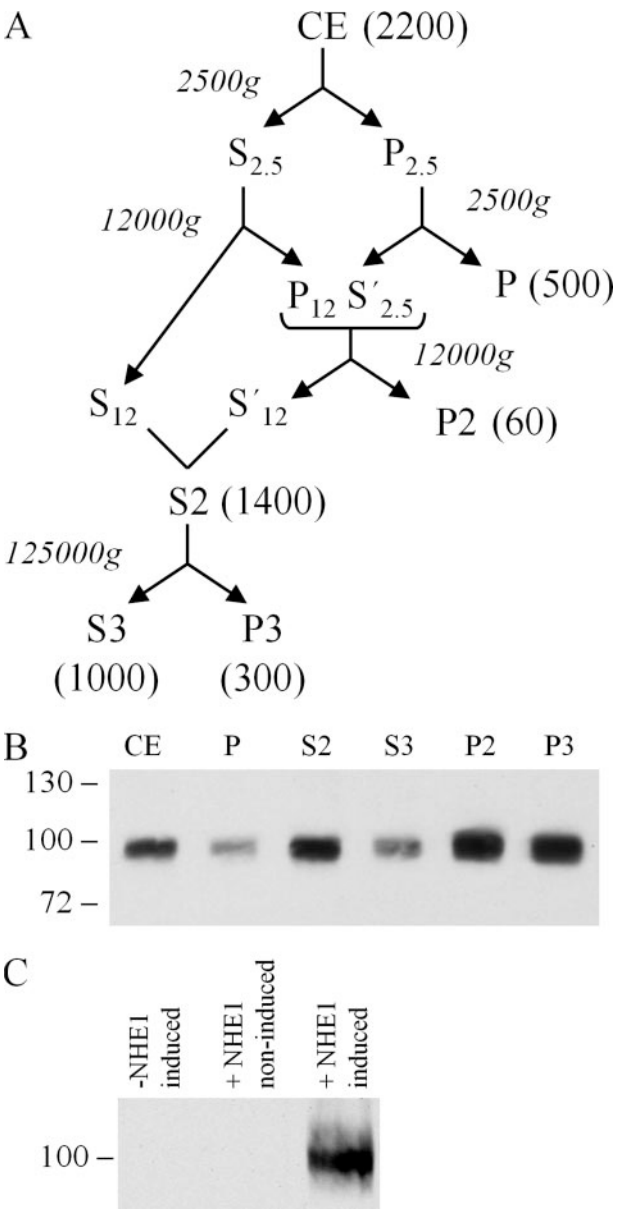

FIGURE 1. **Preparation and characterization of yeast membrane fractions containing hNHE1 (for further details, see "Experimental Procedures").** *A*, schematic diagram of the fractionation procedure with the amounts of total protein from 1 liter of yeast culture indicated in *parentheses* (milligrams). Above, the cell extract (*CE*), supernatants (*S*), and pellets (*P*) are indicated for each stage in the differential centrifugation procedure. *B*, Western blot analysis showing relative amounts of NHE1 at various stages of the fractionation procedure (1.5 μg of protein were loaded for each sample). *C*, Western blot analysis of crude extracts showing expression of hNHE1 specific for *S. cerevisiae* strain w303.1b transformed with the plasmid pYeDP60-hNHE1. Yeast were transformed with either the empty vector pYeDP60 (−NHE1) or the NHE1 vector pYeDP60-hNHE1 (+NHE1), with or without induction for 12 h. hNHE1 was detected with HisProbe-HRP. Molecular mass markers are indicated in kDa.

TABLE 1
Summary of the purification of hNHE1 expressed in *S. cerevisiae*

Fraction[a]	Total protein	hNHE1	hNHE1/ protein	Yield	-Fold purification
	mg	*mg*	*%*	*%*	
CE	2200				
S2	1400				
P3 (Mb)	300	0.9	0.3	100	1
KCl-stripped membranes	130	0.8	0.6	88	2
Ni-NTA purified	0.3	0.2	70	23	233

[a] Values are reported for 1 liter of cell culture.

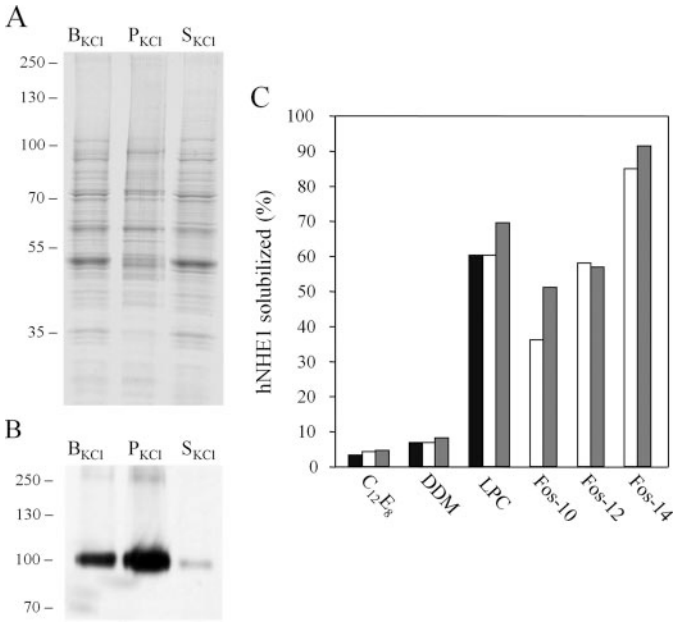

FIGURE 2. **Stripping and detergent solubilization of yeast-expressed hNHE1.** *A*, Coomassie Blue-stained denaturing gel of P3 membrane samples before and after KCl stripping (6 μg of protein were loaded in each lane). Lanes indicate the membrane suspension before stripping (B_{KCl}), and the pellet (P_{KCl}) and the supernatant (S_{KCl}) obtained after stripping and collection of the membranes by centrifugation. Molecular mass markers are indicated in kDa. *B*, Western blot analysis showing relative amounts of NHE1 in the B_{KCl}, P_{KCl}, and S_{KCl} fractions (6 μg of protein were loaded in each lane). Approximately 20% of hNHE1 is lost to the supernatant after KCl stripping and collection of the membranes by centrifugation. hNHE1 was detected with HisProbe-HRP. *C*, solubilization of KCl-stripped membrane fractions with $C_{12}E_8$, DDM, LPC, FC-10, FC-12, and FC-14 at detergent:protein ratios (w:w) of 1:1 (*black bars*), 3:1 (*white bars*), and 5:1 (*gray bars*). Samples were solubilized as described under "Experimental Procedures" and the yield was determined by Western blotting using HisProbe-HRP and quantification of reactive bands. Values are given as the percentage of total hNHE1.

much less hNHE1. From 1L of yeast culture, 20 ml of P3 membrane fraction were obtained at a protein concentration of 15 mg/ml. We used the P3 membrane fraction for all subsequent solubilization and purification steps.

High Ionic Strength Stripping and Solubilization of hNHE1—Prior to solubilization we tested the effect of high KCl treatment to remove peripheral membrane proteins and to enrich the membrane fractions for the hNHE1 protein. The incubation of P3 membranes with 0.7 M KCl removed up to 70% of the protein content (Fig. 2*A*) while not more than 20% of the hNHE1 was lost to the supernatant during this step (Fig. 2*B*). This led to an approximate 2-fold enrichment of hNHE1, and this step proved to be invaluable in improving the subsequent purification by immobilized metal ion affinity chromatography. When this step was omitted, we observed that detergent solubilized-hNHE1 eluted from the Ni-NTA-agarose at low concentrations of imidazole (50 mM). With the inclusion of this step, hNHE1 was retained on the column after low concentration imidazole washes (50 mM) and eluted at high imidazole concentration (250 mM). Therefore, P3 membranes were routinely treated with KCl before solubilization and purification.

Detergents are central to the isolation and solubilization of membrane proteins, yet the selection process remains somewhat empirical. The efficacy of detergents varies with individual proteins and selection of a suitable detergent is important in determining protein yield and in preserving protein function. Consequently a variety of detergents (LPC, $C_{12}E_8$, DDM, FC-10, FC-12, and FC-14) were tested for their ability to solubilize hNHE1 from KCl stripped P3 membranes. Western blotting after removal of insoluble material by centrifugation assessed the solubilization of hNHE1. The results are summarized in Fig. 2*C*. The most efficient solubilization of the hNHE1 protein occurred with the detergents LPC, FC-10, FC-12, and FC-14. The maximum efficiency was 61 and 92% with LPC and FC-14, respectively, and increasing the detergent/protein ratio did not considerably enhance solubilization. Interestingly, increasing the acyl chain length of Fos-choline detergents enhanced solubilization, suggesting that hydrophobic matching may be important in the solubilization of hNHE1. Thus, LPC and FC-14 were suitable detergents that could be used interchangeably in the solubilization and functional preservation of recombinant hNHE1.

Purification of Recombinant hNHE1—Detergent-solubilized membranes were applied to Ni-NTA-agarose, followed by SDS-PAGE and Western blotting to monitor the purification process (Fig. 3). The majority of hNHE1 protein was retained on the column and washing the column with either 10 or 50 mM imidazole only removed trace amounts of the hNHE1. Fractions enriched in hNHE1 eluted at 250 mM imidazole with a purity of ~70% (Fig. 3*A*, *lane E*). The purification achieved approximately a 100-fold enrichment for hNHE1 following a single cycle of binding and elution from the Ni-NTA-agarose. The protein yield after this chromatography step was 0.3 mg/liter (~0.2 mg/liter hNHE1) of culture according to quantification by Amido Black assay and densitometry of Coomassie Blue-stained gels. Further purification of hNHE1 was achieved via calmodulin affinity chromatography. This was designed to take advantage of the presence of a calmodulin binding site on the C-terminal tail of NHE1 (36). In this procedure, the Ni-NTA fractions most enriched in hNHE1 were pooled and incubated with calmodulin-agarose in the presence of calcium, followed by elution with calcium-free buffer. This second purification resulted in removal of many contaminants and produced a more homogeneous protein (≥90%; Fig. 3*C*, *lane E*), based on quantification by densitometry of Coomassie Blue-stained gels. However, the purification procedure was not routinely used because relatively low amounts of purified protein (~0.1 mg/liter) were recovered.

Finally, we wished to examine the glycosylation state of the yeast-expressed hNHE1 by comparing it with NHE1 expressed in mammalian AP1 cells. Our recombinant hNHE1 possessed a similar molecular mass to the de- or partially glycosylated form of NHE1 in AP1 cells (*lower bands*, Fig. 3*D*) (13). This is consistent with expectations based on the N75D mutation that removed the site of *N*-linked glycosylation from the yeast-expressed hNHE1.

Na^+/H^+ Exchange Activity—To confirm that recombinant hNHE1 was functional and could conduct cation exchange, purified hNHE1 was reconstituted into phosphatidylcholine vesicles in the presence of ammonium (NH_4^+) and the fluorescent pH indicator pyranine. Pyranine fluorescence has

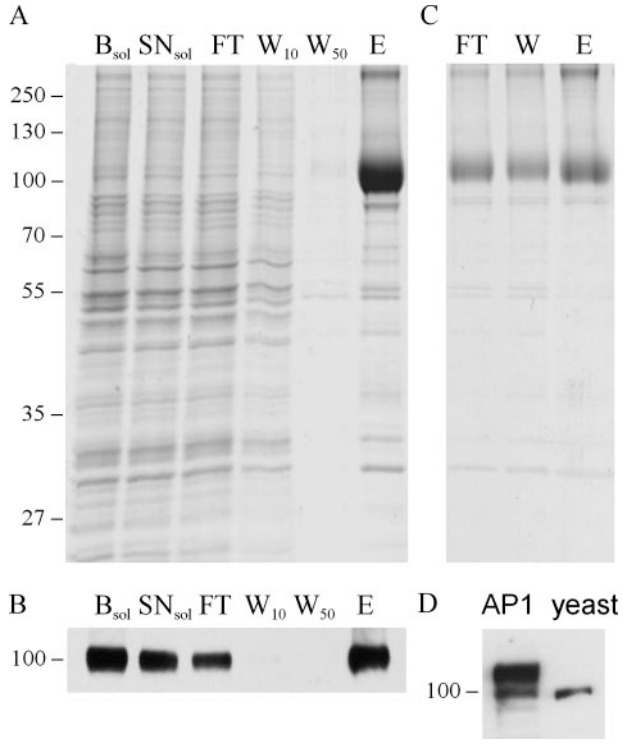

FIGURE 3. **SDS-PAGE and Western blot analysis of the purification of hNHE1.** *A*, Coomassie Blue-stained denaturing gel showing different stages of the Ni-NTA chromatographic purification of hNHE1 (5 μl were loaded for each lane). The starting material was the KCl-stripped membranes shown in Fig. 2*A* (P_{KCl}). The lanes shown above are before solubilization (B_{sol}; 50 ml total volume), supernatant after solubilization (SN_{sol}; 50 ml total volume), flow through (FT; 50 ml total volume), wash with 10 mM imidazole (W_{10}; 10 ml total volume), wash with 50 mM imidazole (W_{50}; 10 ml total volume), and the elution with 250 mM imidazole (E; 2 ml total volume from peak fractions). *B*, Western blot analysis of the different stages of the Ni-NTA chromatographic purification of hNHE1 (3 μl loaded for each, except 0.5 μl for the elution fraction). *C*, further purification of hNHE1 using calmodulin-Sepharose chromatography evaluated by SDS-PAGE and Coomassie Blue staining (10 μl loaded for each). The Ni-NTA chromatography eluate shown in *panel A* was loaded onto the column. The flow through (*lane FT*); wash (*lane W*), and elution (*lane E*) fractions are shown. *D*, Western blot comparing the relative glycosylation states of hNHE1 expressed in mammalian cells (*AP1*) and recombinant hNHE1 purified from *S. cerevisiae* (yeast). In the AP1 lane, the *upper band* is the fully glycosylated form of NHE1 and the *lower band* is the deglycosylated or partially glycosylated form of NHE1. The yeast-expressed hNHE1 co-migrates with the deglycosylated or partially glycosylated form. hNHE1 was detected with HisProbe-HRP. Molecular mass markers are indicated in kDa.

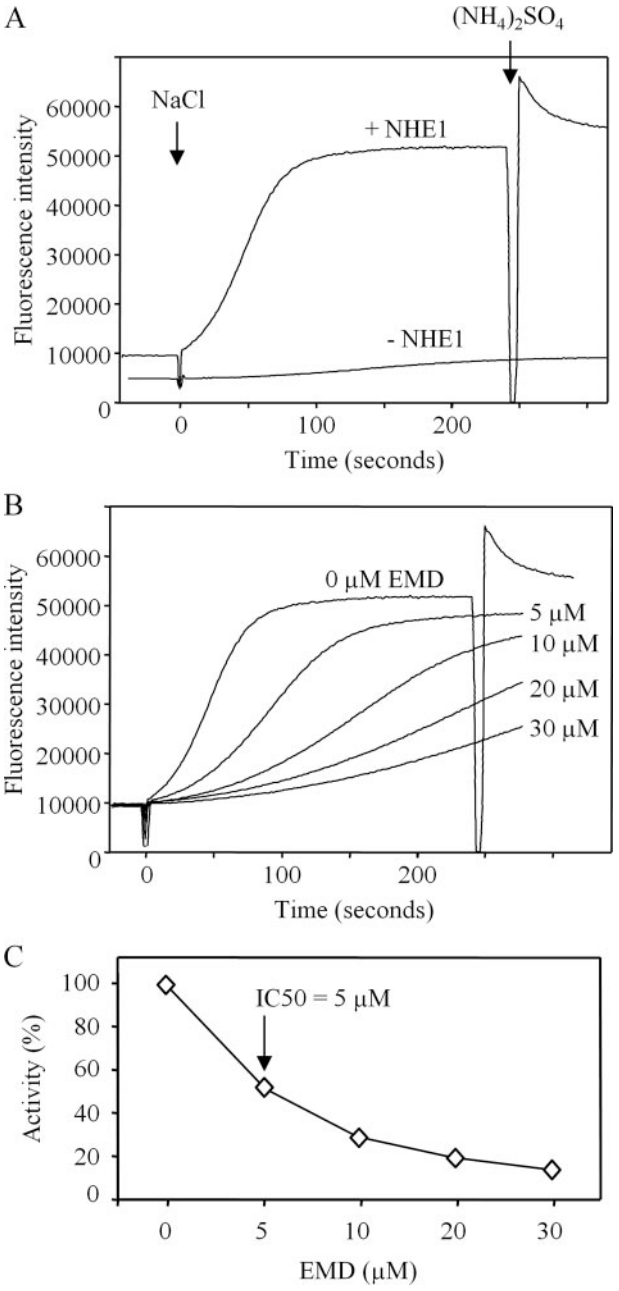

FIGURE 4. **Na^+/H^+ exchange activity of reconstituted hNHE1.** Reconstitution into liposomes was carried out in the absence and presence of hNHE1, in buffer containing ammonium at pH 7.5. An acid-inside pH gradient was created by a 20-fold dilution of proteoliposomes in reconstitution buffer without ammonium at pH 7.5. After 2 min, Na^+/H^+ exchange was initiated by the addition of NaCl. *A*, measurement of Na^+/H^+ exchanger activity of reconstituted proteoliposomes in the absence (−NHE1) or presence (+NHE1) of hNHE1 protein. *B*, effect of preincubation with EMD87580 on NHE1 activity. Inhibition of the Na^+/H^+ exchanger by EMD87580 was measured by preincubating the proteoliposomes in the presence of varying concentrations of EMD87580. After 5 min, NaCl was added and the change in pyranine fluorescence was monitored. *C*, summary of inhibitory effect of EMD87580 on NHE1. The relative hNHE1 activities measured as the change in fluorescence intensity per second for the curves shown in *panel B* were 7400 (control, 0 μM EMD87580), 3856 (5 μM), 2119 (10 μM), 1420 (20 μM), and 1064 (30 μM). The relative hNHE1 activities (% control) were plotted against the concentration of inhibitor (the IC_{50} value for EMD87580 is indicated).

been shown to directly reflect the intravesicular pH (37, 38). Dilution of the proteoliposomes into ammonium-free buffer resulted in acid loading of the vesicles due to outward diffusion of ammonia (NH_3). Efflux of intra-vesicular H^+ in exchange for extravesicular Na^+ was monitored by the increase of pyranine fluorescence upon addition of NaCl. The activity assays showed that hNHE1-containing proteoliposomes mediated rapid cation exchange, compared with a low background of cation exchange by vesicles lacking hNHE1 (Fig. 4*A*). The addition of $(NH_4)_2SO_4$ completely collapsed the cation gradient across the vesicle membranes and resulted in full recovery of pyranine fluorescence. When vesicles were preincubated with the amiloride analog EMD87580, a potent specific NHE1 inhibitor (39), cation exchange activity of the hNHE1 proteoliposomes was inhibited in a dose-dependent manner (Fig. 4*B*). The measured IC_{50} value for hNHE1 inhibition by EMD87580 was 5 μM (Fig. 4*C*), which is similar to the value reported for wild-type hNHE1 expressed in mammalian cells (39).

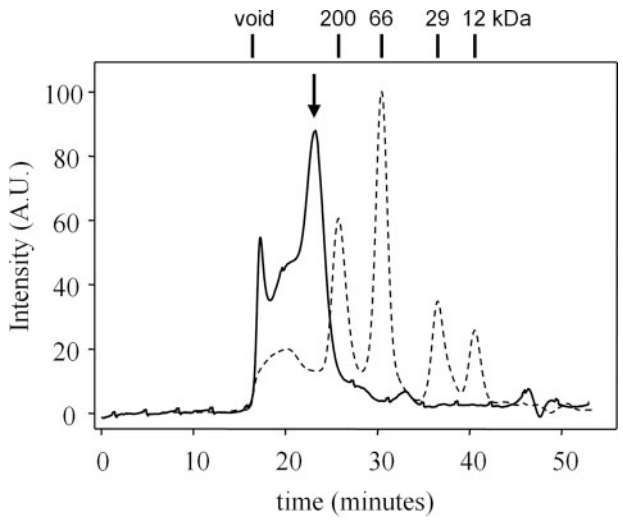

FIGURE 5. **Characterization of purified hNHE1 by size-exclusion chromatography.** The purified hNHE1 was run on a Superdex 200 FPLC column equilibrated with 25 mM HEPES-KOH pH 7.5, 100 mM NaCl, 10% glycerol, 0.05% FC-14. Peaks were identified by their retention time (*solid line*). The elution profile for a series of standard proteins is shown (*dashed line*) and the known molecular weights are indicated. The *arrow* denotes the major hNHE1 peak as confirmed by Western blot analysis (data not shown).

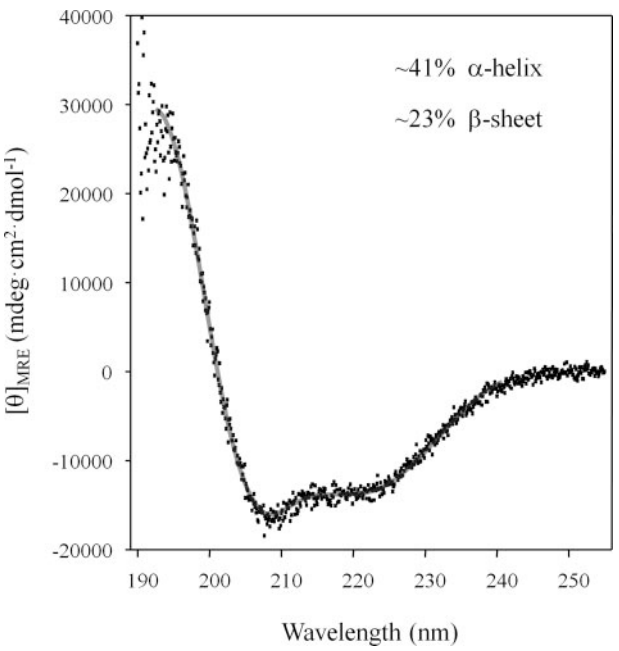

FIGURE 6. **Secondary structure analysis of purified hNHE1.** Far ultraviolet-CD spectra of purified hNHE1 in a buffer of 25 mM phosphate buffer pH 7.5, 10% glycerol, 0.05% FC-14 and recorded at 20 °C. Protein concentration was determined by amino acid analysis and the mean residue ellipticity is given in mdeg × cm^2 × $dmol^{-1}$. The percentage of secondary structure elements was deduced from the ultraviolet-CD spectra using CDPro software (54). Data for three separate experiments are shown (×) plus the curve fit following CDPro analysis (−).

Whereas the EMD87580 sensitivity indicated that we were measuring hNHE1 exchange, we also measured the cation dependence of transport to further confirm the identity of our recombinant protein. Transport was measured over a range of cation concentrations (5–150 mM NaCl, LiCl, and KCl) in the absence and presence of the specific inhibitor EMD87580. The NHE1-specific transport was then reflected in the difference between transport in the absence and presence of the inhibitor. NHE1 carries out sodium- and lithium-stimulated proton transport, but potassium does not compete with sodium for transport and is not an appropriate substrate for NHE1 (40, 41). Our recombinant hNHE1 exhibited sodium-dependent transport that increased rapidly with NaCl concentration and saturated at 50–75 mM NaCl (no observable transport at 5 mM NaCl; 30% transport activity at 25 mM NaCl; 100% transport activity at 75 mM NaCl). Lithium also stimulated transport activity, but the concentration dependence was not characterized. By comparison, there was no measurable potassium-stimulated transport. These results indicate that our recombinant hNHE1 is fully functional, with an inhibitor sensitivity and cation-dependence that is characteristic of this exchanger.

Biophysical and Biochemical Characterization of Recombinant hNHE1 Protein—The oligomeric state of purified hNHE1 was analyzed by size-exclusion chromatography on a Sephadex 200 column (Fig. 5). Purified hNHE1 in detergent (FC-14) was applied to a column pre-equilibrated with the same detergent. The elution profile consisted of two main peaks: a small peak running with the void volume and a large peak with a retention time of 23.2 min indicating a molecular mass in slight excess of 200 kDa. Each peak contained hNHE1 as determined by Western blot analysis (data not shown). Including the FC-14 detergent micelle (108 molecules; aggregation number of FC-14 obtained from Anatrace, Maumee, OH), the approximate molecular mass for an hNHE1 dimer is 233 kDa, consistent with the larger second peak observed in the chromatogram (*arrow* in Fig. 5).

To gain insights into the secondary structure of purified hNHE1 we used CD spectroscopy. The CD spectral profile (Fig. 6) showed two local minima at 208 and 222 nm characteristic of a high α-helical content (42). Analysis of the spectrum indicated that the recombinant hNHE1 contains 41% α-helix, 23% β-sheet, and 36% random coil. These values are consistent with topological predictions of NHE1 that suggest 12 transmembrane helices (43).

Electron Microscopy and Single Particle Reconstruction of hNHE1—Electron micrographs of negatively stained hNHE1 revealed a homogeneous and uniform distribution of particles that were ~100 Å in diameter (Fig. 7*A*). Particle selection yielded 7,930 projections that were grouped by reference-free alignment and classification. Some class averages exhibited 2-fold symmetry (Fig. 7*B*). Fourier common lines approaches implemented in both EMAN and SPIDER were utilized to determine the relative orientations of 44 class averages, which were then combined to generate an initial three-dimensional model. This initial model was used as a starting reference for subsequent rounds of alignment and classification, followed by reference-free orientation determination in EMAN and SPIDER. The final three-dimensional model after imposing 2-fold symmetry (Fig. 7*C*) indicated a resolution of 22 Å, with a fairly even distribution of particle orientations used in the reconstruction (data not shown). The volume shown in Fig. 7*C* (4σ density cutoff) corresponds to a 184-kDa protein, which is exactly twice the mass expected for an hNHE1 monomer. Thus, the reconstruction reveals that recombinant hNHE1 is a dimer.

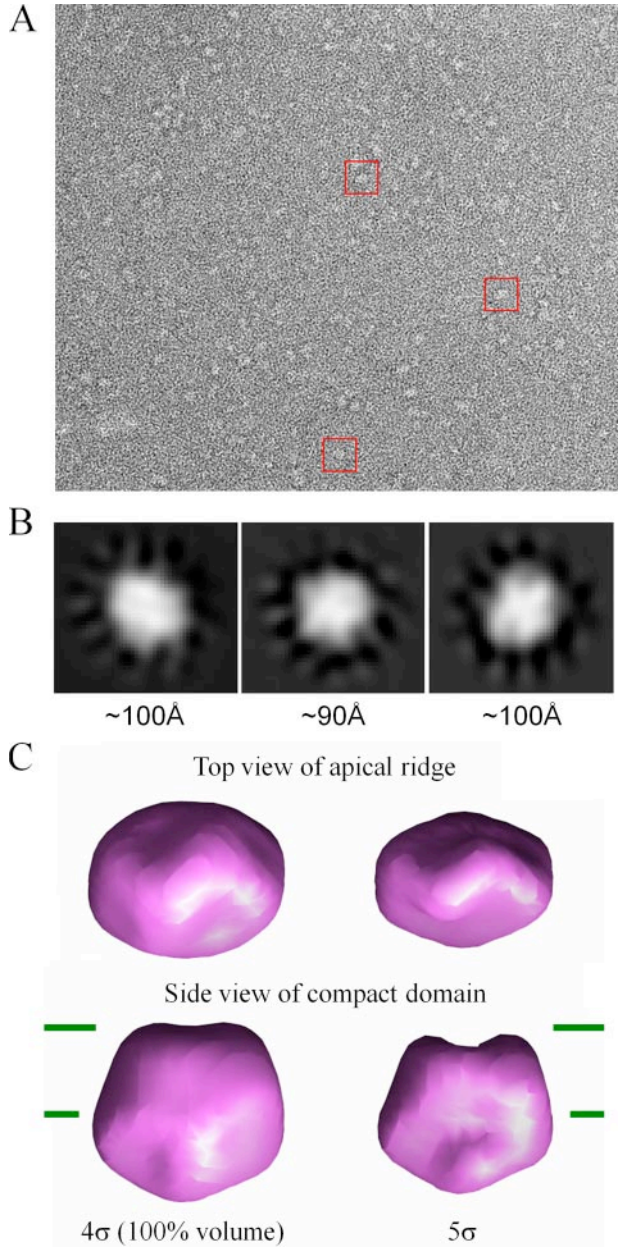

FIGURE 7. **Electron microscopy and three-dimensional reconstruction of recombinant, purified hNHE1.** *A*, electron micrograph of the negatively stained sample, with three particles boxed for clarity. *B*, examples of reference-free two-dimensional class averages indicating a slightly elliptical hNHE1 molecule (with approximate dimensions 100 Å × 100 Å × 90 Å). *C*, molecular surface of hNHE1 at 22-Å resolution showing the "top view" and the "side view" at two density thresholds. The *left half* of the panel is rendered at a density threshold for 100% volume recovery of a hNHE1 dimer. The *bars* delimit the "compact domain", and the "apical ridge" that sits atop this domain.

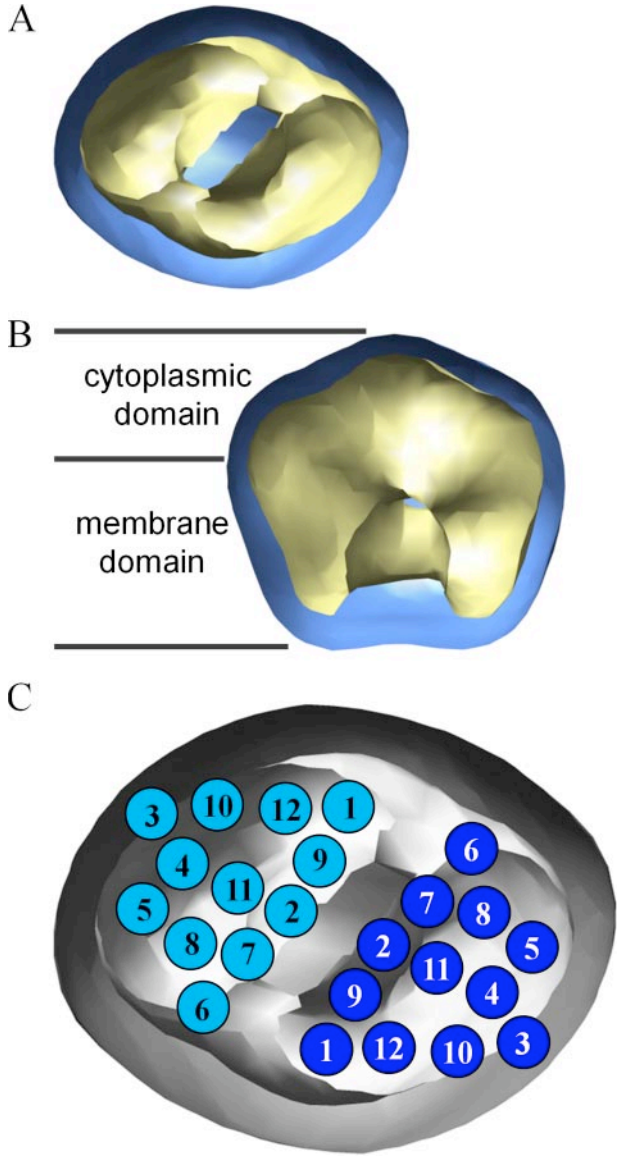

FIGURE 8. **Interpretation of the hNHE1 reconstruction.** *A*, top view of the hNHE1 reconstruction cropped through the middle of the membrane. At higher density thresholds (*yellow surface*), the reconstruction subdivides into two domains, each of which resembles the size and shape expected for an hNHE1 monomer. *B*, side view of the hNHE1 reconstruction cropped perpendicular to the membrane. At higher density thresholds (*yellow surface*), the membrane domain of the reconstruction subdivides while the cytoplasmic domain remains as a continuous density. *C*, based on comparison of the hNHE1 reconstruction and the crystal structure of NhaA (48, 53), the positions of the 12 transmembrane segments of NhaA are superimposed on the reconstruction of the hNHE1 dimer.

This size is consistent with our predictions based on size-exclusion chromatography (Fig. 5), as well as previous studies suggesting that NHE1 is a dimer (44–46).

The hNHE1 reconstruction can be divided into two regions: a compact, globular domain that we assign to the transmembrane domain of hNHE1 and an apical ridge that we assign to the cytoplasmic domain of hNHE1. The relative size of these regions is consistent with their expected molecular mass (58 and 34 kDa, respectively). At higher density thresholds (4.8σ), the globular region of the reconstruction splits into two subdomains (Fig. 8, *A* and *B*). The size and shape of each of these subdomains compares well with the distribution of 12 transmembrane helices expected from hNHE1 topological predictions. The cytoplasmic domain of the hNHE1 reconstruction forms an elongated ridge that sits atop the transmembrane domain. The size of this ridge is consistent with a dimer formed by hNHE1 cytoplasmic domains, each consisting of ~300 amino acids. Unlike the transmembrane domain, which subdivides at higher density thresholds, the apical ridge remains a single continuous domain. This observation suggests extensive contact between cytoplasmic domains in the hNHE1 dimer.

The extensive contact between cytoplasmic domains in the hNHE1 reconstruction is in good agreement with a recent report that the proximal region of the cytoplasmic tail (amino acids 530–580) of hNHE1 has s strong propensity to self-associate (46).

DISCUSSION

Human NHE1 is an important target for the clinical improvement of heart disease, and a number of inhibitors of hNHE1 have been developed for this purpose (11). The molecular structure of hNHE1 would aid the development of therapeutics, yet this structure remains unknown. While the Na^+/H^+ exchangers possess high activity, they are present in very low abundance in mammalian tissues. Therefore, it has not been possible to purify significant amounts of these proteins from native sources for structural characterization. While we have expressed single transmembrane segments of hNHE1 in *E. coli* and characterized them by NMR spectroscopy (3), larger segments containing two or more transmembrane helices have proven refractory to expression. In addition, we have not been successful in the over-production of a yeast Na^+/H^+ exchanger, Sod2, in *E. coli* (14). In an attempt to resolve these problems, we used a yeast expression system to over-produce the hNHE1 protein in amounts suitable for biophysical characterization of the protein. *S. cerevisiae* as an expression system has proven successful with transport proteins of similar overall function and origin (18, 22, 35). We successfully expressed hNHE1 in *S. cerevisiae* in amounts large enough for purification and characterization. Approximately 200 μg of purified protein could be obtained per liter of culture, consistent with the yields obtained for the heterologous expression of other membrane proteins (17, 47). Our data demonstrate that hNHE1 expressed in yeast retains functionality after purification in detergent solution and reconstitution into proteoliposomes. The reconstituted hNHE1 is capable of Na^+-dependent H^+ transport, and can be inhibited by the specific inhibitor EMD87580 (39). Because we expressed hNHE1 with the *N*-linked glycosylation site removed, we confirmed directly earlier suggestions (32, 33) that *N*-linked glycosylation is not essential for cation transport activity.

In these studies, we used detergent-solubilized, purified hNHE1 for biophysical characterization of secondary structure content (CD spectroscopy), oligomeric state (gel filtration chromatography), and low resolution molecular structure (single particle electron microscopy). Analysis of purified hNHE1 by CD spectroscopy demonstrated significant α-helical content, consistent with the predicted topology of 12 transmembrane segments. Based on this analysis and the transport measurements, we were confident that recombinant hNHE1 was properly folded and fully functional. Since there were persistent reports in the literature that hNHE1 exists as a dimer (44, 45), we utilized gel filtration chromatography to address the oligomeric state of the protein in detergent solution. The molecular mass estimated by this technique was in slight excess of 200 kDa, while the predicted molecular weight of our recombinant hNHE1 was 92 kDa. The calculated molecular mass for an hNHE1 dimer was 233 kDa, including 108 detergent molecules in the micelle. It therefore seems likely that the majority of our detergent-solubilized hNHE1 eluted as a dimer by gel filtration chromatography; however, a minor fraction of the protein eluted in the void volume and may form a higher order aggregate or larger micelle.

Last, we used single particle electron microscopy of recombinant hNHE1 to confirm the oligomeric state and to determine the molecular shape of the exchanger. The three-dimensional reconstruction of NHE1 at 22 Å resolution revealed an elongated cytoplasmic domain closely associated with a compact, dimeric transmembrane domain. The overall shape of the transmembrane domain in each hNHE1 monomer is comparable to the only known crystal structure of a Na^+/H^+ exchanger, NhaA from *E. coli* (43, 48), as well as electron crystallographic analyses of two homologous bacterial Na^+/H^+ exchanger dimers, NhaA (49, 50) and MjNhaP1 (51). While this does not ensure that NhaA and NHE1 are comparable, a recent molecular model of NHE1 has been published based on the structure of NhaA (52). These authors used a combined approach of fold recognition, multiple sequence alignments, evolutionary conservation, and published data to construct a model of NHE1. Not surprisingly, the model of NHE1 resembles the structure of NhaA; however, the model was validated by mutagenesis of the NhaA inhibitor binding site as predicted by the NHE1 model. The present comparison of NhaA with NHE1 allows direct insights into the arrangement of the 12 transmembrane segments in our hNHE1 three-dimensional reconstruction. The main predictions that arise from this analysis relate to hNHE1 dimer assembly. First, the cytoplasmic domain of our three-dimensional reconstruction forms an elongated apical ridge that sits atop the transmembrane domains. This suggests a tight, compact interface between cytoplasmic domains that may serve a primary role in dimer stabilization. This is in agreement with earlier suggestions that have shown that the proximal region of the NHE1 cytoplasmic domain has a strong propensity to form a dimer (46). Second, a recent model for the dimeric arrangement of NhaA based on EPR spectroscopy (53) fits well with our hNHE1 reconstruction (Fig. 8*C*). This model makes specific predictions about the transmembrane segments that form the dimer interface, where potential interactions involving transmembrane segments 2, 7, and 9 may help to stabilize the dimer. While these predictions remain unproven for hNHE1, they provide a framework for future structure-function studies.

Acknowledgments—We thank Dr. Paul Scott for assistance with the CD spectroscopy, and we thank Yongsheng Liu for technical assistance.

REFERENCES

1. Fliegel, L. (2005) *Int. J. Biochem. Cell Biol.* **37,** 33–37
2. Sardet, C., Franchi, A., and Pouysségur, J. (1989) *Cell* **56,** 271–280
3. Slepkov, E. R., Rainey, J. K., Sykes, B. D., and Fliegel, L. (2007) *Biochem. J.* **401,** 623–633
4. Wakabayashi, S., Bertrand, B., Shigekawa, M., Fafournoux, P., and Pouyssegur, J. (1994) *J. Biol. Chem.* **269,** 5583–5588
5. Moor, A. N., and Fliegel, L. (1999) *J. Biol. Chem.* **274,** 22985–22992
6. Karmazyn, M., Sawyer, M., and Fliegel, L. (2005) *Curr. Drug Targets Cardiovasc. Haematol. Disord.* **5,** 323–335
7. Cardone, R. A., Casavola, V., and Reshkin, S. J. (2005) *Nat. Rev. Cancer* **5,** 786–795

8. Avkiran, M. (2001) *Basic Res. Cardiol.* **96,** 306–311
9. Zeymer, U., Suryapranata, H., Monassier, J. P., Opolski, G., Davies, J., Rasmanis, G., Linssen, G., Tebbe, U., Schroder, R., Tiemann, R., Machnig, T., and Neuhaus, K. L. (2001) *J. Am. Coll. Cardiol.* **38,** 1644–1650
10. Lazdunski, M., Frelin, C., and Vigne, P. (1985) *J. Mol. Cell. Cardiol.* **17,** 1029–1042
11. Avkiran, M., and Marber, M. S. (2002) *J. Am. Coll. Cardiol.* **39,** 747–753
12. Mentzer, R. M., Jr. (2003) *Circulation* **108,** 2723 (abstract)
13. Slepkov, E. R., Rainey, J. K., Li, X., Liu, Y., Cheng, F. J., Lindhout, D. A., Sykes, B. D., and Fliegel, L. (2005) *J. Biol. Chem.* **280,** 17863–17872
14. Dibrov, P., Young, P. G., and Fliegel, L. (1998) *Mol. Cell Biochem.* **182,** 125–132
15. Long, S. B., Campbell, E. B., and Mackinnon, R. (2005) *Science* **309,** 897–903
16. Parcej, D. N., and Eckhardt-Strelau, L. (2003) *J. Mol. Biol.* **333,** 103–116
17. Jidenko, M., Nielsen, R. C., Sorensen, T. L., Moller, J. V., le Maire, M., Nissen, P., and Jaxel, C. (2005) *Proc. Natl. Acad. Sci. U. S. A.* **102,** 11687–11691
18. Lenoir, G., Menguy, T., Corre, F., Montigny, C., Pedersen, P. A., Thines, D., le Maire, M., and Falson, P. (2002) *Biochim. Biophys. Acta* **1560,** 67–83
19. Flegelova, H., Haguenauer-Tsapis, R., and Sychrova, H. (2006) *Biochim. Biophys. Acta* **1760,** 504–516
20. Flegelova, H., and Sychrova, H. (2005) *FEBS Lett.* **579,** 4733–4738
21. Montero-Lomeli, M., and Okorokova Facanha, A. L. (1999) *Biochem. Cell Biol.* **77,** 25–31
22. Sekler, I., Kopito, R., and Casey, J. R. (1995) *J. Biol. Chem.* **270,** 21028–21034
23. Schiestl, R. H., and Gietz, R. D. (1989) *Curr. Genet.* **16,** 339–346
24. Nakamura, N., Tanaka, S., Teko, Y., Mitsui, K., and Kanazawa, H. (2005) *J. Biol. Chem.* **280,** 1561–1572
25. Gebreselassie, D., Rajarathnam, K., and Fliegel, L. (1998) *Biochem. Cell Biol.* **76,** 837–842
26. Sreerama, N., and Woody, R. W. (2004) *Protein Sci.* **13,** 100–112
27. Rieder, C. V., and Fliegel, L. (2002) *Am. J. Physiol.* **283,** H273–H283
28. Kaplan, R. S., and Pedersen, P. L. (1985) *Anal. Biochem.* **150,** 97–104
29. Schaffner, W., and Weissmann, C. (1973) *Anal. Biochem.* **56,** 502–514
30. Ludtke, S. J., Baldwin, P. R., and Chiu, W. (1999) *J. Struct. Biol.* **128,** 82–97
31. Frank, J., Radermacher, M., Penczek, P., Zhu, J., Li, Y., Ladjadj, M., and Leith, A. (1996) *J. Struct. Biol.* **116,** 190–199
32. Counillon, L., Pouyssegur, J., and Reithmeier, R. A. (1994) *Biochemistry* **33,** 10463–10469
33. Haworth, R. S., Frohlich, O., and Fliegel, L. (1993) *Biochem. J.* **289,** 637–640
34. Pompon, D., Louerat, B., Bronine, A., and Urban, P. (1996) *Methods Enzymol.* **272,** 51–64
35. Jahn, T., Dietrich, J., Andersen, B., Leidvik, B., Otter, C., Briving, C., Kuhlbrandt, W., and Palmgren, M. G. (2001) *J. Mol. Biol.* **309,** 465–476
36. Bertrand, B., Wakabayashi, S., Ikeda, T., Pouyssegur, J., and Shigekawa, M. (1994) *J. Biol. Chem.* **269,** 13703–13709
37. Venema, K., Gibrat, R., Grouzis, J. P., and Grignon, C. (1993) *Biochim. Biophys. Acta* **1146,** 87–96
38. Venema, K., Quintero, F. J., Pardo, J. M., and Donaire, J. P. (2002) *J. Biol. Chem.* **277,** 2413–2418
39. Ding, J., Rainey, J. K., Xu, C., Sykes, B. D., and Fliegel, L. (2006) *J. Biol. Chem.* **281,** 29817–29829
40. Kleinman, J. G., Harig, J. M., Barry, J. A., and Ramaswamy, K. (1988) *Am. J. Physiol.* **255,** G206–G211
41. Jean, T., Frelin, C., Vigne, P., Barbry, P., and Lazdunski, M. (1985) *J. Biol. Chem.* **260,** 9678–9684
42. Saxena, V. P., and Wetlaufer, D. B. (1971) *Proc. Natl. Acad. Sci. U. S. A.* **68,** 969–972
43. Wakabayashi, S., Pang, T., Su, X., and Shigekawa, M. (2000) *J. Biol. Chem.* **275,** 7942–7949
44. Fliegel, L., Haworth, R. S., and Dyck, J. R. B. (1993) *Biochem. J.* **289,** 101–107
45. Fafournoux, P., Noel, J., and Pouysségur., J. (1994) *J. Biol. Chem.* **269,** 2589–2596
46. Hisamitsu, T., Pang, T., Shigekawa, M., and Wakabayashi, S. (2004) *Biochemistry* **43,** 11135–11143
47. Sarramegna, V., Talmont, F., Demange, P., and Milon, A. (2003) *Cell Mol. Life Sci.* **60,** 1529–1546
48. Hunte, C., Screpanti, E., Venturi, M., Rimon, A., Padan, E., and Michel, H. (2005) *Nature* **435,** 1197–1202
49. Williams, K. A., Geldmacher-Kaufer, U., Padan, E., Schuldiner, S., and W., K. (1999) *EMBO J.* **18,** 3558–3563
50. Williams, K. A. (2000) *Nature* **403,** 112–115
51. Vinothkumar, K. R., Smits, S. H., and Kuhlbrandt, W. (2005) *EMBO J.* **24,** 2720–2729
52. Landau, M., Herz, K., Padan, E., and Ben-Tal, N. (2007) *J. Biol. Chem.* **282,** 37854–37863
53. Hilger, D., Polyhach, Y., Padan, E., Jung, H., and Jeschke, G. (2007) *Biophys. J.* **93,** 3675–3683
54. Sreerama, N., and Woody, R. W. (2000) *Anal. Biochem.* **287,** 252–260